## NUMERICAL AND EXPERIMENTAL STUDY OF THE FLOW OVER A SIMPLE BUILDING

Tomáš Kopáček\* and Luděk Beneš<sup>+</sup> and Milan Jirsák<sup>-</sup>

\* ČVUT, Faculty of Mechanical Engineering, Department of Technical Mathematics, Karlovo nám. 13, Praha 2, 12135

+ Institute of Thermomechanics AS CR, Dolejškova 5, Praha 8, 18200

- ARTI a.s, Department of Low Speed Aerodynamics, Beranových 130, Praha-Letňany

#### Introduction

This contribution presents a study of turbulent flow over a simple building. We considered a building with a flat roof and a building with a double pitched roof. The main goal was to compare our numerical results computed at the Department of Technical Mathematics with experimental data measured in a wind tunnel at ARTI.

#### Mathematical and numerical method

To model incompressible viscous turbulent flow over a complex geometry in 2D, the system of RANS equations completed by the  $k - \omega$  TNT model was considered. Using the method of artificial compressibility, we start with the two dimensional system

$$\Gamma W_t + F_x + G_y = \nu (R_x + S_y),$$

where  $\nu = \nu_M + \nu_T$ ,  $\nu_M$  and  $\nu_T$  denotes molecular and turbulent viscosity, respectively. W = $(p, u, v)^T$  is the vector of unknowns,  $\Gamma = diag(1/\beta^2, 1, 1)$  is a diagonal matrix, F and G are two-dimensional flux vectors and R, S are viscous fluxes, i.e.

$$F = (u, u^2 + p, uv)^T, \quad R = (0, u_x, v_x)^T, G = (v, uv, v^2 + p)^T, \quad S = (0, u_y, v_y)^T.$$

The  $k - \omega$  TNT model is based on two transport equations for k (turbulence kinetic energy) and  $\omega$  (specific dissipation rate) which are coupled with the RANS equations.

$$\begin{aligned} \frac{\partial k}{\partial t} + u_j \frac{\partial k}{\partial x_j} &= \tau_{ij}^R \frac{\partial u_i}{\partial x_j} - \beta^* k \omega + \frac{\partial}{\partial x_j} \left[ \left( \nu + \sigma^* \nu_T \right) \frac{\partial k}{\partial x_j} \right] \\ \frac{\partial \omega}{\partial t} + u_j \frac{\partial \omega}{\partial x_j} &= \alpha \frac{\omega}{k} \tau_{ij}^R \frac{\partial u_i}{\partial x_j} - \beta \omega^2 + \frac{\partial}{\partial x_j} \left[ \left( \nu + \sigma \nu_T \right) \frac{\partial \omega}{\partial x_j} \right] + \frac{1}{2} \omega \max(k_x \omega_x + k_y \omega_y, 0), \end{aligned}$$
where

where

$$\alpha = \frac{5}{9}, \quad \beta^* = 0.09, \quad \beta = \frac{5}{6}\beta^*, \quad \sigma^* = \frac{2}{3}, \quad \sigma = \frac{1}{2}, \quad \nu_T = \frac{k}{\omega}$$

To complete the system the Boussinesq hypothesis is used:

$$\tau_{ji}^R = -2\nu_T S_{ij},$$

where  $\tau_{ji}^R$  are the so called Reynolds stresses and  $S_{ij}$  are the rate of deformation tensor. For more details see e.g. [2].

Numerical discretization has been done by the finite volume method with piecewise linear reconstruction (PLR) limited by Barth–Jespersen limiter and the AUSM scheme used for numerical fluxes. The viscous fluxes have been discretised in central way on a dual mesh. The incurred system of ODR equations have been solved by the second order TVD Runge-Kutta method.

$$\iint_{\Omega_{i}} \int_{t^{n}}^{t^{n+1}} \left[ \Gamma \mathbf{W}_{t} + \mathbf{F}_{x} + \mathbf{G}_{y} - \nu \left( \mathbf{R}_{x} + \mathbf{S}_{y} \right) \right] dt d\Omega_{i} = 0$$
$$\frac{dW_{i}}{dt} = -\frac{\Delta t}{|\Omega_{i}|} \sum_{j=1}^{N_{i}} \left( \mathcal{F}_{ij}^{AUSM} + \mathcal{F}_{ij}^{vi} \right) \mathbf{n}_{ij} \Delta l_{ij}$$
$$\mathcal{F}_{ij}^{AUSM} = \left[ u_{n} \left( \begin{array}{c} 1 \\ u \\ v \end{array} \right)_{L/R} + p \left( \begin{array}{c} 0 \\ n_{x} \\ n_{y} \end{array} \right) \right] \Delta l_{ij}$$

where  $\Delta t$  is the time step,  $|\Omega_i|$  is the area of control volume  $\Omega_i$ ,  $\Delta l_{ij}$  is the length of the face common to the  $i^{th}$  and  $j^{th}$  control volumes,  $\mathbf{n}_{ij}$  denotes the outer unit normal vector to the face,  $\mathcal{F}_{ij}^{AUSM}$  stands for the AUSM flux and  $\mathcal{F}_{ij}^{vi}$  for the viscous flux through the face, see [1]. In order to increase the accuracy of the scheme, the PLR is used in the following form

$$\begin{split} \tilde{\mathbf{w}}_{L} &= \mathbf{w}_{L} + \psi \left( \delta_{L}^{T} \cdot \nabla w_{L} + \frac{1}{2} \delta_{L}^{T} \cdot \mathbb{H} \cdot \delta_{L} \right) \\ \tilde{\mathbf{w}}_{R} &= \mathbf{w}_{R} - \psi \left( \delta_{R}^{T} \cdot \nabla w_{R} + \frac{1}{2} \delta_{R}^{T} \cdot \mathbb{H} \cdot \delta_{R} \right) \\ \end{array}$$

where  $\mathbb{H}$  is the Hesian. The symbol  $\psi$  denotes a suitable limiter. In our computation the Barth-Jespersen limiter was used, see [3].

#### Validation of the applied code

A test case involving turbulent flow around a flat board [3] has been used to validate the code. The value of kinetic viscosity in this case was  $\nu_M = 3.5 \cdot 10^{-7}$ . The velocity on the inlet boundary was set to u=0.2. Figure 1 schematically illustrates the computational domain. The following figure 2 shows the behaviour of friction coefficient  $C_f$  with clearly visible transition from laminar to turbulent regime.

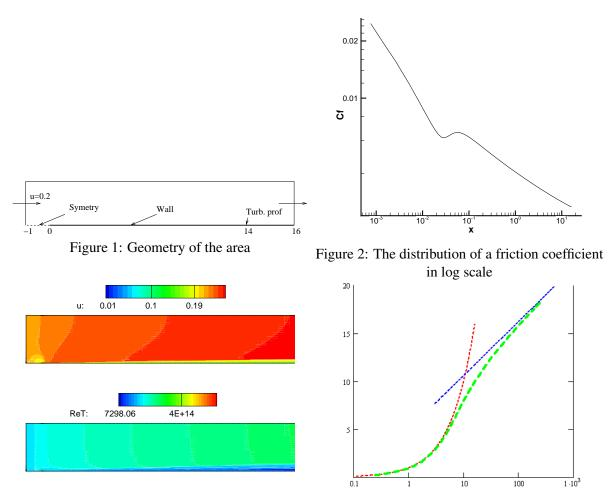


Figure 3: The stream-wise velocity component u Figure 4: The comparison of the computed (up) and the distribution of the turbulent Reynolds turbulent profile (green) with the theoretical profile number (below) (red, blue)

In figure 3 one can see the flowfied of turbulent Reynolds number and velocity u. The last figure shows the comparison of analytically and numerically obtained velocity distribution through turbulent boundary layer, where good agreement between experimental and numerical data can be observed.

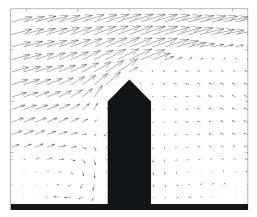


Figure 5: PIV measurement–velocity flow field close to the double piched building

Figure 6: PIV measurement-velocity flow field close to the flat building

#### Numerical and experimental results

The main goal of this work was to obtain numerical results and to compare them with the experimental data measured by the ARTI. The experiment was carried out in a tunnel for simulation of the turbulent boundary layer (BLWT). Several measurements for flows over different geometries were undertaken, namely flow over the double pitched roof and the flat roof.

Nowadays we have done numerical simulation over the flat roof building. The streamlines and the absolute velocity obtained by numerical simulation are shown in figure 8.

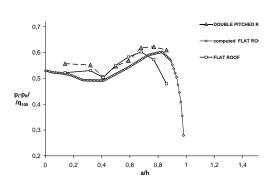


Figure 7: The comparison of the computed and measured presure distribution on the front face of building

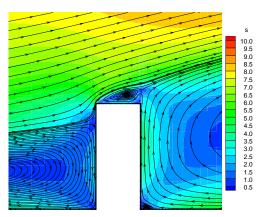


Figure 8: The flat roof building - the streamtraces and the absolute velocity s

#### Conclusion

In figure 7, a comparison of the pressure coefficients obtained by numerical and experimental methods are in good agreement and so we can say that the used numerical schema is proper for this type of tasks. However, distorted mesh and complex phenomena arising near the building influence negatively convergence of the method, therefore it was necessary to decrease the CFL coefficient to 0.1.

### Acknowledgment

The financial support for the present project is partly provided by the Research Plan MSM No.6840770003 and the project of the Grant Agency of the Czech Republic No. 205/06/0727.

# References

- Vierendeeles J., Riemslagh K., Dick E.: A Multigrid Semi-implicit Line-method for Viscous Incompressible and Low-Mach-Number Flows on High Aspect Ratio Grids, *Journal of Computational Physic 154, p.310-314, 1999*
- [2] Wilcox D.C. Turbulence Modeling for CFD, DCW Industries
- [3] Kopáček T.: Numerické řešení vazkého nestlačitelného proudění, *Diploma thesis (in czech) ČVUT*, 2007
- [4] Jirsák M., Zachoval D., Kopáček T.: Wind Tunnel Modelling of Ventilation and Infiltration Boundary Condition, *ARTI in Prague*, 2006
- [5] Fuka V., Brechler J.: 2D model interakce proudění s pevnými překážkami. Colloqium FLUID DYNAMICS 2006 (Jonas, Uruba, eds.), Inst. of Thermomechanics, Acad. of Sci., Prague, 2006,35– 38.